Effective processing of the first broadband 3D marine vibrator data acquired in the North Sea

Arash JafarGandomi[1], Sebastian Holland[1], Kara Howard[1], Tiexing Wang[1], Thomas Elboth[1]*
1. Shearwater Geoservices

Summary

We present the result of processing and imaging of the marine vibrator (MV) Alpha-test, which was recently successfully completed over the permanent monitoring system of the Johan Sverdrup field in the North Sea. The Alpha-test includes the acquisition of a 3D swath of data using a single MV and several test lines using a two-unit source array covering 3-150Hz. The preliminary result of processing and imaging of these data produced images comparable to the legacy airgun array acquisition. Despite the much lower level of energy emitted by the MV with respect to the airgun array of the legacy data, comparable images were obtained. Our results clearly show the realistic possibility of employing the MV for the acquisition of broadband seismic data at large scales.

Effective processing of first broadband 3D marine vibrator data acquired in the North Sea

Introduction

The high-precision signal control of the marine vibrator (MV) allows for novel strategies in survey design (Laws *et al*., 2019). Recently several of the MV's capabilities and their benefits for enhanced data acquisition, effective processing and optimized spatial wavefield sampling have been discussed (JafarGandomi et. al., 2023). Over the last few years there have been some 2D field trials of different marine vibrator technologies tested with limited output frequency ranges of below 100Hz (Teyssandier & Sallas, 2019; Alfaro et. al., 2023, Harnar Singh & Zawawi, 2023). Here on, we present the first broadband (3-150Hz) 3D alpha-test of the marine vibrator, which was successfully carried out in the summer of 2023 over the Johan Sverdrup oil field situated in the North Sea, about 140km west of Stavanger, Norway (Elboth et al., 2024). This field is operated by Equinor ASA, with partners AkerBP ASA, TotalEnergies EP Norge AS, and Petoro AS. The water depth in the area is around 120 meters. In the following sections the acquired data will be briefly described, and then the key processing steps applied to the 3D datasets will be discussed. The migrated images of MV data are then compared with the images obtained from the legacy airgun array. At the end some of the key acquisition differences between the MV used for this test and the airgun array of the legacy survey are discussed.

Data Acquisition

During the Alpha test several test lines (narrow pink swath in Figure 1) as well as a full 3D source carpet swath (wide green swath in Figure 1a) were acquired. The test included single MV lines covering 3-150Hz as well as split frequency, double-unit MV array lines covering 3-25Hz with a low-frequency band (LB) unit and 25-150Hz with the high-frequency band unit (HB). Two ultra-low-frequency test lines covering 1-8Hz were also acquired. The 3D swath was acquired using a single-unit MV covering 3-150Hz. In this study the initial processing results of a selected test line (dashed line in Figure 1a) as well as the 3D swath are described. The processing of other test lines is ongoing and will be presented in the future.

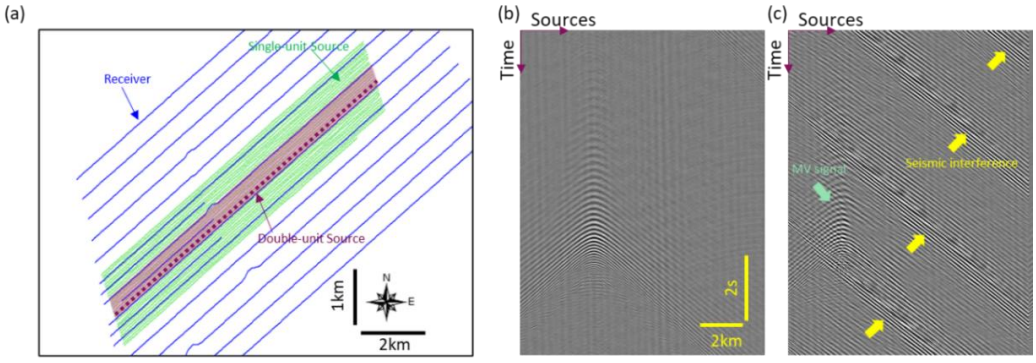

Figure 1 *a) The source and receiver location for the MV alpha test. b) and c) sample common-source-gathers acquired with 10s sweeps covering 3-150Hz.*

In our MV acquisition the source emits acoustic energy (sweeps) continuously. The3D swath used a 10s non-linear up-sweep with phase modulation of [0°, 90°, 0°, 90°, …] for subsequent sweeps. This allows for efficient residual sweep noise attenuation, as shown by Laws et al. (2019). Because of continuous sweeping by the moving source, the concept of source-point as used for airgun acquisitions is not directly applicable. However, we associate source-point locations to a fixed pre-defined position along each sweep e.g., the starting point. With the 10s sweep and a vessel's speed of 4.5knots a nominal source-spacing of 25m is achieved. Figure 1a depicts the distribution of sources for the 3D swath and associated receivers used for data processing. The receiver spacing along the PRM cables is 50m and the distance between neighboring receiver lines varies between 200m and 400m. Figure 1b and 1c depict two examples of common-source gathers from the single-unit test, one of which is contaminated with seismic interference (SI) from an airgun acquisition conducted around 35km away. This SI is further described in the discussion section.

Data processing

The strategy followed in the processing of this marine vibrator data is to convert the MV data acquired by a continuously emitting moving source to equivalent impulsive source data. This means that migration and any other post-processing step remain the same between MV and airgun data. The first stage in the processing of recorded multi-component data is to form the common-receiver gathers based on the nominal source-point locations. In this stage it is important to ensure enough record length is considered for the gathers due to the long source-signature, i.e. sweep, which needs to be deconvolved.

As discussed by (Telling et. al., 2023) estimation of notional source (NS) signatures with high accuracy is essential to effective deconvolution. The MV is equipped with accelerometers mounted on the radiators as well as near field hydrophones (NFHs). We have previously shown that either or both of these measurements may be used for NS estimation. Here we examined all options and noticed that the estimated sweeps when using accelerometers alone were very similar to the sweeps from joint inversion. Hence for the sake of processing efficiency we used the NS estimated from the accelerometer measurements alone. Both P- and Z-components were processed, and the component rotation and calibrations were applied deterministically to the data. At the early stage of processing an approximate sweep deconvolution was carried out as a 1D trace-by-trace operation which removes the phase-encoding from the signal belonging to each record. This is done in order to facilitate data windowing and de-blending. The source motion, which is a time and frequency-dependent effect, remains in the data. After windowing, a global pilot sweep with the same frequency-function-of-time behaviour as the emitted sweep is then convolved with the data before correcting for source motion, free-surface ghost, interpolation, de-blending and re-datuming to a desired datum. Note that all these steps are applied in the common-receiver domain. Figure 2a and 2b show examples of a raw and processed common-receiver-gather, respectively. The impact of phase modulation and splitting frequencies between the two units is clear on the frequency-wavenumber (*f-k*) spectra in Figure 2c.

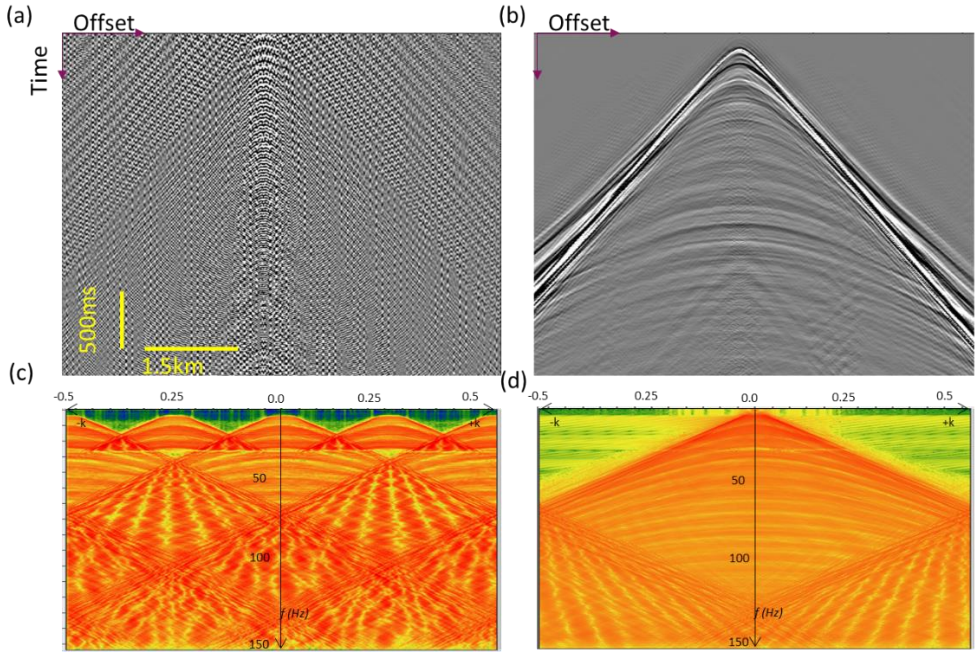

Figure 2 *a) Raw and b) processed common-receiver-gathers acquired with a MV source array containing one low-band and one high-band unit. c) and d) are corresponding f-k spectra. The wavenumber axes shows normalised wavenumber for 12.5m trace spacing.*

The gather shown in Figure 2 is from one of the test lines acquired using two MV units simultaneously, a LB (3-25Hz) towed at 15m depth and HB (25-150Hz) towed at 5m depth. The sweep lengths were 10s and 5s for LB and HB, respectively. The boat speed of 4.5knots led to 25m and 12.5m source spacing for the LB and HB, respectively. The data are then processed to 12.5m trace spacing (Figure 2b). Figure 3 demonstrates two sample common-source-gathers from the 3D swath test acquired using

a single MV unit towed at 5m emitting 3-150Hz with a 10s sweep, giving 25m source spacing. Phase modulation was also applied in this case. The two selected gathers in Figure 3a, one of which is contaminated with SI, show the result after 1D sweep deconvolution and the corresponding gathers in Figure 3b are the results after full processing inclusive of de-ghosting, re-datuming de-blending and source-motion correction.

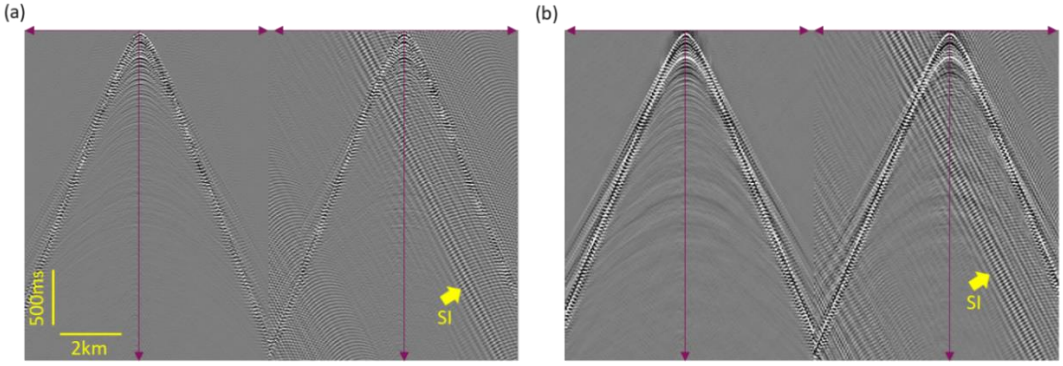

Figure 3 *a) Sample common-source-gathers from the 3D swath after 1D sweep deconvolution and b) after full processing (de-ghosting, de-blending, re-datuming and source-motion correction).*

The processed P- and Z-components are then used for up-down wavefield separation and deconvolution (UDD). The processed gathers were then migrated using Kirchhoff pre-stack depth migration. For comparison, the legacy data acquired by triple-source airgun (1800in^3) was also processed in parallel and sent through the same migration. The source carpet for the legacy data was tailored to be the same as that of the MV acquisition. No matching or synchronization has been applied to either of the datasets.

Figure 4a and 4b show the migrated UDD results from the legacy airgun and MV acquisitions, respectively. Two sets of close-ups from the middle (Figures 4c & 4d) and deeper parts (Figures 4e & 4f) of the images are also shown. Comparison of the MV and the airgun images shows strong similarity in both the character and detail of structures down to the base of target formations at around 2.5km (Figures 4d). Furthermore, even the major dipping event extending to 4km (indicated by thick yellow arrow in Figure 4b) is nicely imaged and can easily be tracked on both airgun and MV images.

Discussions

While Figure 4 shows a good correspondence between the images obtained from the airgun and MV acquisition, it is important to note that the emitted energy of the MV source used here was much lower than for the corresponding airgun array. Based on the calculation of far-field signature for vertical incidence and 10s record, which equates to one sweep emission with MV (25m source spacing) and two airgun firing (12.5m source spacing), the MV emitted about 14.1dB re uPa^2.m^2.s less energy compared to the legacy airgun acquisition. This affects the signal-to-noise ratio especially in the deeper parts (Figure 4b). Furthermore, one of the key differences between the MV and legacy acquisition was the strong seismic interference (SI) at the time of MV acquisition, which was absent on the legacy data. The removal of SI is currently being investigated with promising initial results. However, it was not applied to the preliminary processing results shown here. Nevertheless, the processed images are comparable to the SI-free legacy image. Further investigation of the impact of SI for different source types, i.e. impulsive source and continuous sweeping, will be the subject of our future research.

Conclusions

The MV Alpha test was successfully completed, including acquiring a 3D swath of data using a single unit covering 3-150Hz and several test lines using a two-unit source array. The test was conducted over the Johan Sverdrup PRM system in the North Sea. The preliminary processing and imaging of these data shows images comparable to the legacy airgun array acquisition. This achievement is despite a much lower level of energy emitted by the MV as well as the presence of strong SI noise on MV data. The full processing of these data is still ongoing and further results will be presented in the near future.

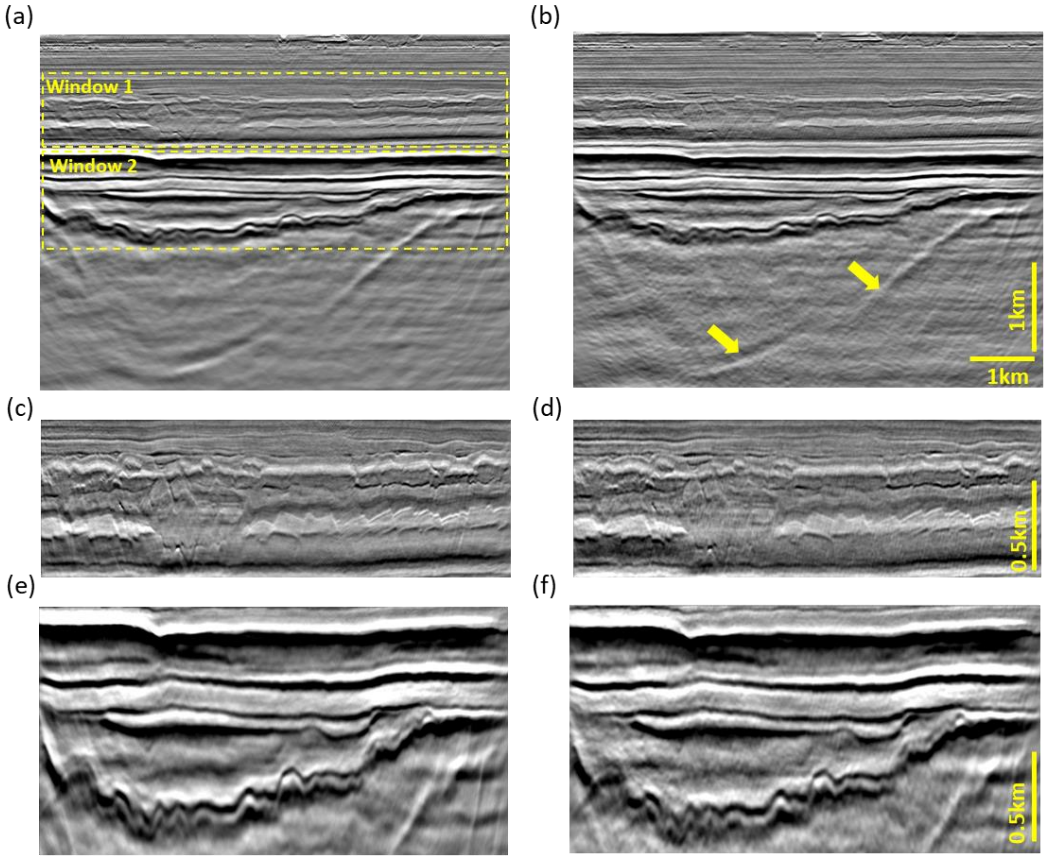

Figure 4. *Pre-stack depth migrated images of the UDD results for a) legacy airgun acquisition and b) for the 3D swath of MV. c) and d) are close-ups corresponding to window 1 highlighted in (a) and, e) and f) close-ups corresponding to window 2 highlighted in (a).*

Acknowledgements

We would like to thank Shearwater GeoServices and our project partners and sponsors; AkerBP ASA, Equinor ASA and Vår Energy ASA, and the Johan Sverdrup license operator Equinor ASA and partners Petoro AS, Aker BP ASA, and TotalEnergies EP Norge AS for their permission to record the data over the field and publish these results.

References

Alfaro, R., Secker, S., Zamboni, E., Cozzens, A., Henderson, N., Jenkerson, M., Nechayuk, V., Johnson, G. and Karran, J., [2023]. Validation of an Alternative Seismic Source: The Integrated Projector Node Marine Vibrator Pilot Seismic Survey. In *84th EAGE Annual Conference and Exhibition.*

JafarGandomi, A., Nath, A. and Grion, S., [2023]. August. Value of marine vibrators for effective frequency-dependent spatial sampling of seismic wavefield. In *Third International Meeting for Applied Geoscience & Energy (IMAGE pp. 182-186).*

Laws, R.M., Halliday, D., Hopperstad, J-F., Gerez, D., Supawala, M., Özbek, A., Murray, T., Kragh, E. [2019]. Marine vibrators: the new phase of seismic exploration. *Geophysical Prospecting*. 67,1443-1471.

Telling, R.H., JafarGandomi, A., Laws, R.M., Grion, S., [2023]. Estimating the signature of a marine vibrator by joint inversion of hydrophone and accelerometer measurements, In *84th EAGE Annual Conference and Exhibition.*

Teyssandier, B. and Sallas, J.J., [2019]. The shape of things to come-Development and testing of a new marine vibrator source. *The Leading Edge*, 38(9), pp.680-690.

Singh, T.H. and Zawawi, M.B., 2023, June. Transition Zone Exploration: A Relentless Effort in Search for the Most "Ideal" Source. In *84th EAGE Annual Conference and Exhibition.*

Elboth, T., Evensen, A, Jafargandomi, A. and Laws R.M., [2024]. The first Broadband Marine 3D vibrator survey. Submitted to the *85th EAGE Annual Conference and Exhibition*.